Available online at www.sciencedirect.com
ScienceDirect
Catalysis Today 120 (2007) 363–367
CATALYSIS TODAY
www.elsevier.com/locate/cattod

H_2 uptake and synthesis of the fluorinated Li-dispersed nickel oxide nanotubes

Jin Bae Lee, Soon Chang Lee, Sang Moon Lee, Hae Jin Kim *

Energy Nano Material Team, Korea Basic Science Institute, Daejeon 305-333, Republic of Korea

Available online 9 November 2006

Abstract

Aligned Li-dispersed nickel oxide nanotubes were prepared using $LiNO_3$, $Ni(NO_3)_2{\cdot}6H_2O$ and an anodic aluminum oxide (AAO) template for potential applications in H_2 storage. The nanotubes were characterized by X-ray diffraction (XRD), scanning electron microscopy (SEM) and transmission electron microscopy (TEM). The nickel(II) oxide nanotubes obtained had a trigonal structure with a uniform length, 40–50 nm in wall thickness and 200 ± 10 nm in the outer diameter. The external surface of the nanotubes was modified by fluorination. The level of H_2 adsorption was determined using the gravimetric method. The fluorinated Li-dispersed nickel oxide nanotubes showed a 0.06 wt% and 1.65 wt% increase in weight due to H_2 adsorption under an equilibrium pressure of 47 atm at 298 K and 77 K, respectively.

Keywords: Hydrogen adsorption; Nickel oxide nanotube; Anodic aluminum oxide (AAO) template; Fluorination; Lithium

1. Introduction

There has been increasing demand for efficient and clean alternatives to fossil fuels. This is expected to become more pronounced in the future with many automotive companies having announced the production of commercially available fuel cell vehicles as soon as 2010 [1].

There are many problems with H_2 storage, e.g. technologies and materials. In addition, the H_2 adsorption mechanism is not completely understood. There are storage technologies for H_2 such as high-pressure vessels, liquefied H_2, metal hydrides, carbon nanotubes, etc. [2–5]. Among these, carbon nanotubes have shown various H_2 storage capacities ranging from 0 wt% to 67.55 wt% [6,7]. However, there is some doubt regarding the cyclability of these storage capacities. Recently, the limitation of H_2 storage using carbon nanotubes only has been recognized. Therefore, the surface modification of nanotubes has attracted increased attention [8]. Many studies have been made using inorganic nanomaterials for H_2 storage [9]. Metal nanostructured materials, such as metal nanoparticles, nanowires and nanoarrays have been studied extensively on account of their interesting electronic and optical properties [10–13] and potential applications in nanodevices [14–16]. There are other materials to adsorb or intercalate H_2 such as layered structures (hexagonal, trigonal, and orthogonal), high surface area nanostructures ($LiAlO_2$) and high porosity nanostructure (zeolites).

A template technique is a promising method for synthesizing nanosized materials with ordered structures. In particular, many researchers have fabricated a variety of one-dimensional nanomaterials, e.g., nanotubes, nanowires, or nanorods using uniform and straight nanochannels of an anodic aluminum oxide film as a template [17].

This paper reports the novel synthesis and characterization of nickel oxide nanotubes and Li-dispersed nickel oxide nanotubes prepared using a porous AAO template. The hydrogen adsorption capacity was characterized.

Anodic aluminum oxide (AAO) membranes are frequently used to aid the formation of such structures inside their straight, cylindrical and uniformly sized high-density channels [18]. This method entails the synthesis of a desired material within the pores of a microporous membrane, which have cylindrical pores with monodisperse diameters. A tubule or fibril of the desired material is obtained within each pore. Because the aspect ratios of the nanostructures prepared using this method can be controlled, this template approach is proving to be a versatile method for synthesizing many nanomaterials [19].

The syntheses of nanostructures such as carbon nanotubes by chemical vapor deposition (CVD) [20], sodium nanotubes

* Corresponding author. Tel.: +82 42 865 3953; fax: +82 42 865 3963.
E-mail address: hansol@kbsi.re.kr (H.J. Kim).

0920-5861/$ – see front matter © 2006 Elsevier B.V. All rights reserved.
doi:10.1016/j.cattod.2006.09.010

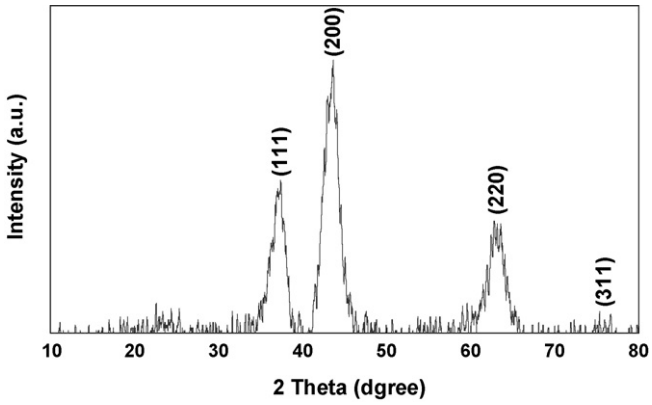

Fig. 1. XRD patterns of the nickel oxide nanotubes.

formed inside AAO [21] and $LiMn_2O_4$ [22] nanowire arrays, have been studied using the AAO template.

Nickel oxide is widely used as a catalyst [23–25] and electrode [26–29]. The NiO electrode has a high resistivity, which is a serious drawback for practical applications to supercapacitors [30]. The use of nickel oxide mixed catalysts has also been reported in the partial oxidation of methane [24], the selective oxidation of propane [25] and oxidative dehydrogenation of ethane [26]. In addition, Ni-metal alloy has been investigated for use in H_2 storage [31–33].

2. Experimental

2.1. Preparation of nickel oxide nanotubes

Analytical grade reagents were used without further purification. The nickel oxide nanotubes were prepared by using nickel(II) nitrate hexahydrate ($Ni(NO_3)_2{\cdot}6H_2O$, Aldrich 98%) and an AAO template (Anodisc 47, Whatman). A 0.2 mol of $Ni(NO_3)_2{\cdot}6H_2O$ was dissolved in 100 mL of distilled water. A 1.8 g of the AAO templates were placed in the nickel nitrate solution at room temperature for 4 h. The Ni-AAO template was then dried at 313 K in a vacuum for 4 h and at 373 K in air for 4 h. The AAO template was etched away by dissolving the Ni-AAO templates in a 1 M NaOH solution for 6 h. The as-synthesized green precipitate was filtered, washed several times with distilled water and then dried at 373 K in air for 2 h. The product was then calcined at 773 K in air for 2 h.

2.2. Preparation of Li-dispersed nickel oxide nanotubes

A 1.38 g of $LiNO_3$ and 5.82 g of $Ni(NO_3)_2{\cdot}6H_2O$ were dissolved in 100 mL of distilled water. A 1.8 g of the AAO template was immersed in a Li–Ni water solution. The subsequent processes were identical to the upper processes.

The structure and morphological properties of the nickel nanotubes were characterized using several techniques. The phase purity of the products was examined by X-ray diffraction (XRD) using a BRUKER D8-advance X-ray diffractometer with Cu Kα radiation ($\lambda = 1.5418$ Å). The operation voltage and current was maintained at 40 kV and 40 mA, respectively. The morphology was examined using field emission scanning electron microscopy (FE-SEM, Hitachi S-4700 SEM). The micro/nanostructure of the products was further examined using field emission transmission electron microscopy (FE-TEM, JEOL JEM2100F).

2.3. Experimental setup for hydrogen adsorption capacity

The H_2 adsorption capacity of the Li-dispersed nickel oxide nanotubes was performed in an experimental apparatus (MSB-AD-H, BEL Japan Inc.) and a magnetic suspension microbalance (MSB, Rubotherm) using the gravimetric method. Only the main steps of the complete experimental procedure (outgassing, determination of the volume of the sample and adsorption isotherm measurement) are reported. The adsorbed gases and water were removed by heating the nanotubes at 353 K under a pressure of $<10^{-3}$ Pa and for 12 h. After the pretreatment, the sample was transferred to a microbalance. The sample volume was determined by measuring the force exerted by an inert gas (helium) on the sample in order to perform the buoyancy effect correction. The procedure for measuring the H_2 adsorption kinetics was quite simple. Small quantities of H_2 were admitted to the adsorption chamber. After each admission, an equilibrium test was performed on the mass and pressure. This procedure was completely automated. The pressure and temperature were stored in a data file and the apparent adsorbed mass was corrected to allow for the buoyancy effect. The H_2 adsorption measurements were performed at room temperature and 77 K under 47 atm.

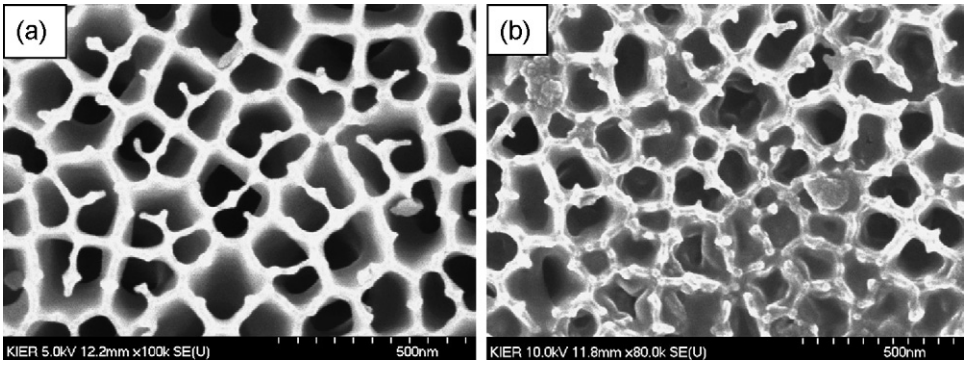

Fig. 2. SEM images of (a) AAO template and (b) Ni-AAO template.

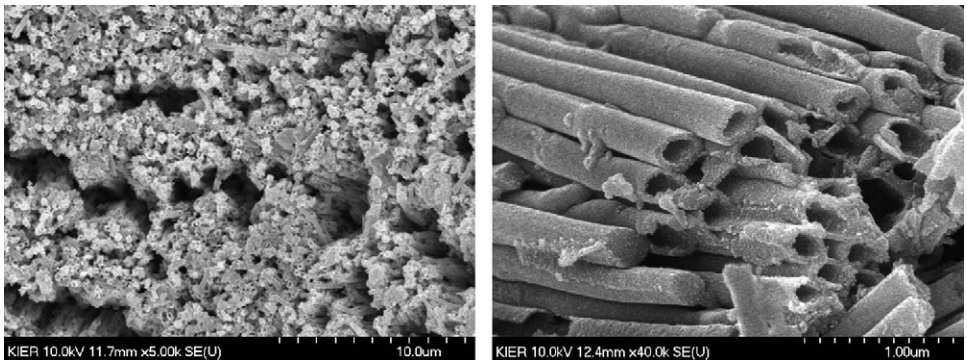

Fig. 3. SEM images of the nickel oxide nanotubes.

3. Results and discussion

3.1. XRD and SEM analysis

Fig. 1 shows the XRD patterns of the nickel oxide nanotubes. Four diffraction peaks, which were assigned to (1 1 1), (2 0 0), (2 2 0) and (3 1 1) planes, were clearly distinguishable, and nickel(II) oxide was indexed to the trigonal structure (space group $R\bar{3}m$, $a = 4.145$ Å, $b = 4.145$ Å, $c = 4.145$ Å, $\alpha = \beta = \gamma = 90.47^{\circ}$).

Fig. 2 shows the SEM images of the raw AAO template and the AAO template coated with Ni. The AAO template had an average pore diameter and thickness of 200 nm and 60 μm, respectively. An upside-view of the AAO template in Fig. 2(a) shows that the nanochannels were highly ordered, parallel to each other and had smooth inner walls as well as a uniform diameter. This suggests that a similar ordered array of NiO nanotubes can be prepared using AAO as the template. The AAO template covered with Ni precursor was sometimes blocked, as shown in Fig. 2(b).

Fig. 3 shows the scanning electron microscope (SEM) images of the nickel oxide nanotubes obtained. The nanotubes were uniformly distributed with a length ranging from 1 μm to 50 μm. The length of the nickel oxide nanotubes was <60 μm

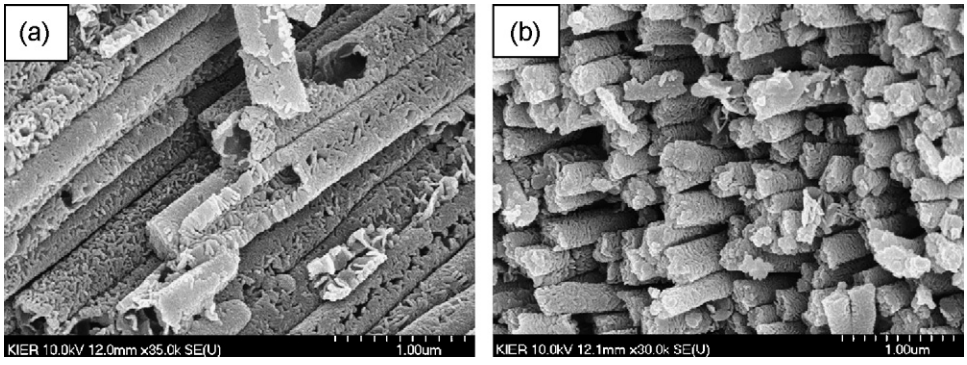

Fig. 4. SEM images of the Li-dispersed nickel oxide (a) nanotubes and (b) nanorods.

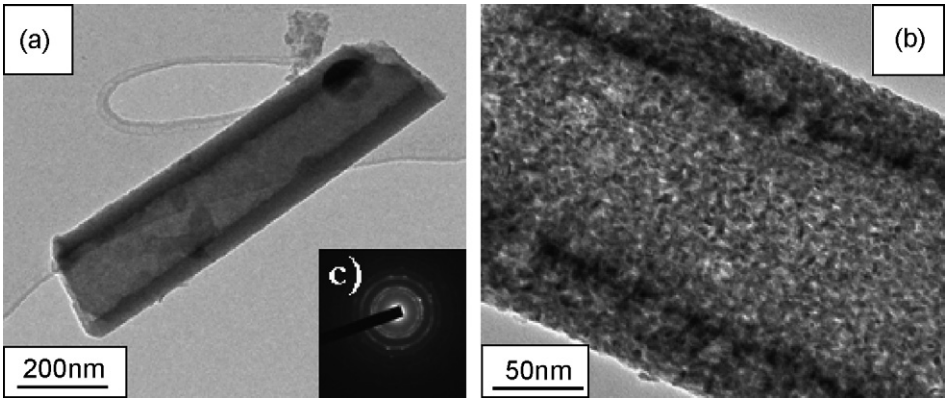

Fig. 5. (a) and (b) TEM images of the nickel oxide nanotubes and (c) SAD pattern.

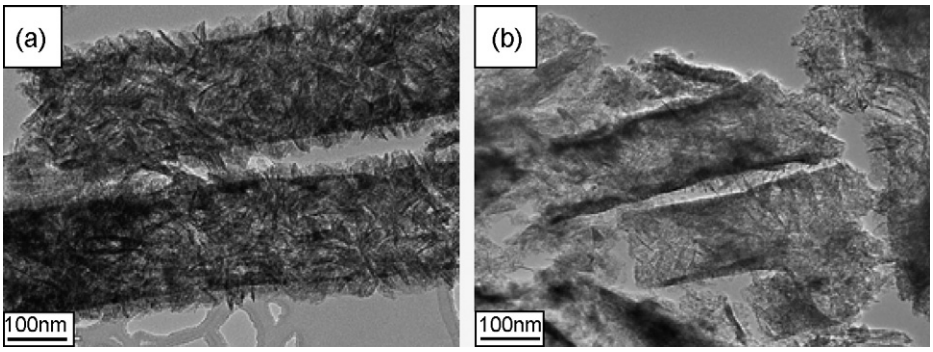

Fig. 6. TEM images the Li-dispersed nickel oxide of (a) nanorods and (b) nanotubes.

of the average AAO template. Most of nickel oxide nanotubes had an open end and a closed end partially.

Fig. 4 shows SEM images of Li-dispersed nickel oxide nanotubes and nanorods. The wall of the Li-dispersed nickel oxide nanotube was composed of nanoflakes. The size of the nanoflakes was similar to the wall thickness of the nanotube. The nanotubes had a partly closed end and the nanoflakes appeared tangled.

3.2. TEM analysis

TEM was used to provide further insight into the morphology and microstructure details of the nickel oxide nanotubes. Fig. 5 shows TEM images of the nickel oxide nanotubes with a pore diameter $d = 200 \pm 10$ nm. The nickel oxide nanotubes appeared to be cylindrical with a wall thickness of approximately 40–50 nm. It was reported that the diameter of the Li-dispersed nickel oxide nanotubes is in accordance with the pore diameter of the AAO template [34,35]. The nickel oxide nanotubes consisted of a continuous, multilayered nanoparticle array. Some partly broken nanotubes were observed. Fig. 5(c) shows the corresponding selected-area electron diffraction (SAED) pattern taken from these nanotubes.

Fig. 6 shows TEM images of the Li-dispersed nickel oxide nanotubes and nanorods. The Li-dispersed nickel oxide nanotubes had an incomplete nanotube wall compared with pure nickel oxide nanotubes, as shown in Fig. 6(b). Spaces between the nanoflakes were observed because a section of the nanorods was thinly packed with nanoflakes.

3.3. Fluorination of Li-dispersed nickel oxide nanotubes

The surface was modified by the brief fluorination of Li-dispersed nickel oxide nanotubes. Prior to fluorination, the Li-dispersed nickel oxide nanotubes were dried at 473 K in vacuum for 2 h. The pretreated sample was placed into a Ni boat in the fluorine reaction chamber made from Ni and stainless steel 316 SS (17Cr–12Ni–2.5Mo) in order to prevent erosion. Mixed F_2 and N_2 gases were introduced into the chamber (pressure ration of 1:9), with under a pressure of 1 bar at room temperature for 30 min. N_2 gas plays a role in removing residual oxygen and moisture. After the reaction, the chamber was again evacuated to 10^{-2} Torr, and nitrogen gas was refilled prior to extracting the sample.

3.4. H_2 adsorption

The adsorption experiment was performed using the gravimetric method. An absolute pressure indicator was used to measure the equilibrium pressure. The adsorption volume measured by the gravimetric method showed the influence of buoyancy according to the density of the atmosphere fluid.

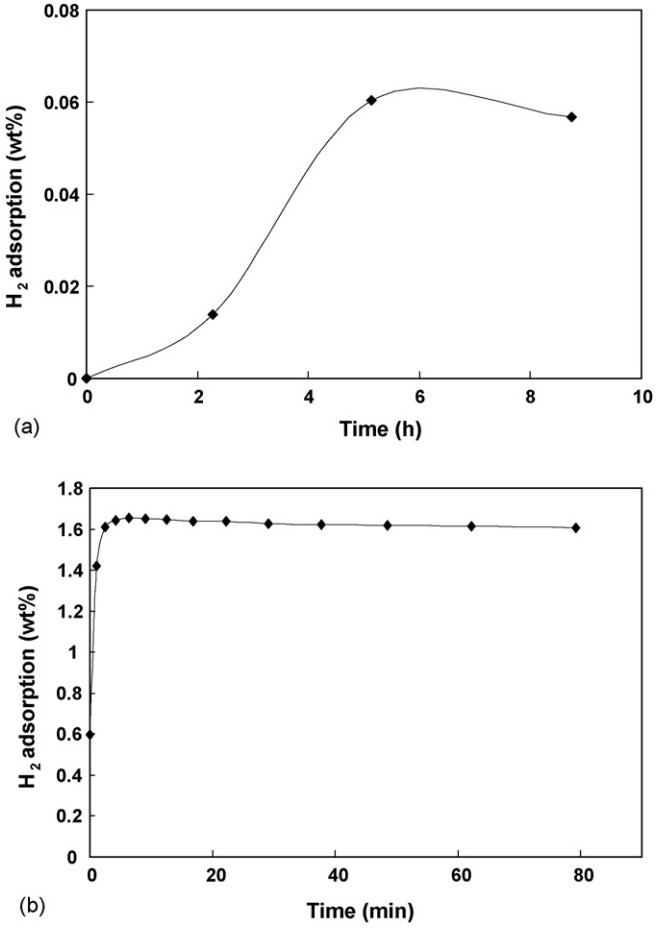

Fig. 7. H_2 adsorption of Li-dispersed nickel oxide nanotubes (a) at 298 K and (b) 77 K under 47 atm.

Therefore, the values of the actual direct-vision balance do not correspond to the amount adsorbed. The amount of H_2 adsorption was calculated as follows:

$$\text{fluid exclusion volume} = V_d + \frac{W_s}{d_s} + \frac{W_a}{d_a} \quad (1)$$

$$\text{the adsorbed amount} = W_c + \text{fluid exclusion volume} \times d_f \quad (2)$$

where V_d is the volume of the upper coupling device and the hook, W_s, W_a and W_c are the weight of the sample basket, the weight of the adsorbent and the weight change of the sample, respectively. d_s, d_a and d_f refer to the true density of the sample basket, the true density of the adsorbent and the density of the fluid, respectively. This calculation procedure was completely automated by a personal computer.

As can be seen in Fig. 7, the H_2 adsorption capacities of Li-dispersed nickel oxide nanotubes at 298 K and 77 K could be determined. The adsorption graphs show that the level of H_2 adsorption increased with time. However, after 6 h and 0.1 h, respectively, the level of H_2 adsorption on the Li-dispersed nickel oxide nanotubes became saturated. Fig. 7(a) and (b) indicate that H_2 adsorption on the Li-dispersed nickel oxide nanotubes at relatively higher temperature took a relatively long time to reach saturation.

The fluorinated Li-dispersed nickel oxide nanotubes showed a 0.06 wt% and 1.65 wt% increase in weight at 298 K and 77 K under an equilibrium pressure of 47 atm, respectively.

4. Conclusions

This study demonstrated a simple procedure for fabricating nanotubes using a $Ni(NO_3)_2{\cdot}6H_2O$ and AAO template. The isolated nickel oxide nanotubes were easily obtained by removing the AAO template with NaOH. Nickel oxide nanotubes were composed of a continuous nanoparticle array. The wall thickness and outer diameter of the cylindrical nickel oxide nanotubes was approximately 40–50 nm and 200 ± 10 nm, respectively. It was observed that the diameter of the Li-dispersed nickel oxide nanotubes was in accordance with the pore diameter of the AAO template. The XRD patterns revealed the nickel(II) oxide nanotubes to have a trigonal structure. The fluorinated Li-dispersed nickel oxide nanotubes showed a 0.06 wt% and 1.65 wt% increase in weight under an equilibrium pressure of 47 atm at 298 K and 77 K, respectively.

Acknowledgements

This Research was performed for the Hydrogen Energy R&D Center, one of the 21st Century Frontier R&D Program, funded by the Ministry of Science and Technology of Korea.

References

[1] A.M. Swayad, D.M. Antonelli, Adv. Mater. 16 (2004) 765.
[2] N. Takeichi, H. Senoh, T. Yokota, H. Tsuruta, K. Hamada, H.T. Takesita, H. Tanaka, T. Kiyobayashi, T. Takano, N. Kuriyama, Int. J. Hydrogen Energy 28 (2003) 1121.
[3] P.J. Mueller, J.C. Batty, R.M. Zubrin, Cryogenics 36 (1996) 815.
[4] V. Guther, A. Otto, J. Alloys Compd. 293–295 (1999) 889.
[5] A.C. Dillon, K.M. Jones, T.A. Bekkedahl, C.H. Kiang, D.S. Bethune, M.J. Heben, Nature 386 (1997) 377.
[6] A. Chambers, C. Park, R.T.K. Baker, N.M. Rodriguez, J. Phys. Chem. B 102 (22) (1998) 4253.
[7] M. Hirscher, M. Becher, M. Haluska, U. Dettlaff-Weglikowska, A. Quintel, G.S. Duesberg, Y.M. Choi, P. Downes, M. Hulman, S. Roth, I. Stepanek, P. Bernier, Appl. Phys. A 72 (2001) 129.
[8] S.M. Lee, S.C. Lee, J.H. Jung, H.J. Kim, Chem. Phys. Lett. 416 (2005) 251.
[9] S.H. Lim, J. Luo, Z. Zhong, W. Ji, J. Lin, Inorg. Chem. 44 (2005) 4124.
[10] T. Goodson, O. Varnavski, Y. Wang, Int. Rev. Phys. Chem. 23 (2004) 109.
[11] P.V. Kamat, J. Phys. Chem. B 106 (2002) 7729.
[12] Y.H. Cheng, S.Y. Cheng, Nanotechnology 15 (2004) 171.
[13] J.P. Novak, L.C. Brousseau III, F.W. Vance, R.C. Johnson, B.I. Lemon, J.T. Hupp, D.L. Feldheim, J. Am. Chem. Soc. 122 (2000) 12029.
[14] D.H. Cobden, Nature 409 (2001) 32.
[15] Y. Cui, C.M. Lieber, Science 291 (2001) 851.
[16] A.J. Haes, S.L. Zou, G.C. Schatz, R.D. Van Duyne, J. Phys. Chem. B 108 (2004) 6961.
[17] K. Matsui, B.K. Pradhan, T. Kyotani, A. Tomita, J. Phys. Chem. B 105 (2001) 5682.
[18] L.S. Wang, C.Y. Lee, H.T. Chiu, Chem. Commun. 15 (2003) 1964.
[19] X.H. Li, W.M. Liu, H.L. Li, Appl. Phys. A 80 (2005) 317.
[20] Y.C. Sui, D.R. Acosta, J.A. Gonzalez-Leon, A. Bermudez, J. Feuchtwanger, B.Z. Cui, J.O. Flores, J.M. Saniger, J. Phys. Chem. B 105 (2001) 1523.
[21] L.S. Wang, C.Y. Lee, H.T. Chiu, Chem. Commun. 15 (2003) 1964.
[22] Y.K. Zhou, C.M. Shen, J. Huang, H.L. Li, Mater. Sci. Eng. B 95 (2002) 77.
[23] F. Basile, G. Fornasari, F. Trifiro, Catal. Today 64 (2001) 21.
[24] N. Fujikawa, K. Wakui, K. Tomita, N. Ooue, W. Ueda, Catal. Today 71 (2001) 83.
[25] A. Kaddouri, R. Anouchinsky, C. Mazzocchia, L.M. Madeira, M.F. Portela, Catal. Today 40 (1998) 201.
[26] T. Fukui, S. Ohara, M. Naito, K. Nogi, Powder Technol. 132 (2003) 52.
[27] X. Liu, X.G. Zhang, Electrochim. Acta 49 (2004) 229.
[28] S.W. Park, J.M. Choi, E. Kim, S. Im, Appl. Surf. Sci. 244 (2005) 439.
[29] A. Aronin, G. Abrosimova, S. Bredikhin, K. Matsuda, K. Meada, M. Awano, J. Am. Ceram. Soc. 88 (2005) 1180.
[30] J.Y. Lee, K. Liang, K.H. An, Y.H. Lee, Synth. Metals 150 (2005) 153.
[31] W.H. Liu, J. Alloys Compd. 404/406 (2005) 694.
[32] W.K. Hu, Y.S. Zhang, D.Y. Song, P.W. Shen, Int. J. Hydrogen Energy 21 (1996) 651.
[33] W. Liu, H. Wu, Y. Lei, Q. Wang, J. Wu, J. Alloys Compd. 252 (1997) 234.
[34] L. Kim, S.M. Yoon, J. Kim, J.S. Suh, Synth. Metals 140 (2004) 135.
[35] Y. Zhou, C. Shen, H. Li, Solid State Ionics 146 (2002) 81.